

Design of a TCP-like Smart Charging Controller for Power Quality in Electrical Distribution Systems

Ammar Alyousef
University of Passau
Passau, Bavaria, Germany
Ammar.Alyousef@uni-Passau.de

Hermann de Meer
University of Passau
Passau, Bavaria, Germany
demmer@uni-Passau.de

ABSTRACT

The increase in Electric Vehicles (EV) penetration may add a significant amount of load to the power grid potentially causing several challenges like overloading of assets and big voltage drops on feeder lines. Overcoming those challenges will be hard because of the variability and unpredictability of EV loads, namely, the lack of information on when, where, for how long or how fast charging processes of EVs would take place. However, the EV extra load had arguably not been taken into account when the distribution grid was designed originally. In addition, expanding the distribution and transmission capacity is a very costly and long process. Hence, it is necessary to adopt a smart EV charging approach to address the issues of peak load and power quality. This work focuses on proposing and evaluating a new smart EV charging controller inspired by the slow start mechanism of the Transmission Control Protocol (TCP) on the Internet. The controller is a part of a distributed smart charging architecture and responds to indication signals regarding the grid state in real time. The indication process adopts a traffic light model and is performed in a distributed way at the grid connection point of each individual Charging Station (CS). Thanks to the notification mechanism, the controller is able to deal with the overloading of assets and keeps the voltage within the allowed boundaries as predefined by the grid operator. The voltage control considers not only the CS but also predetermined remote points.

CCS CONCEPTS

• **Networks** → **Network resources allocation**; • **Computer systems organization** → **Real-time system architecture**; • **Hardware** → **Smart grid**.

KEYWORDS

Distributed Smart Charging, Power Quality, Electric Vehicle, Charging Station, Assets Overloading, Voltage Control, Traffic Light Model, Transmission Control Protocol

ACM Reference Format:

Ammar Alyousef and Hermann de Meer. 2019. Design of a TCP-like Smart Charging Controller for Power Quality in Electrical Distribution Systems. In *e-Energy '19: Proceedings of the Tenth ACM International Conference on*

Permission to make digital or hard copies of all or part of this work for personal or classroom use is granted without fee provided that copies are not made or distributed for profit or commercial advantage and that copies bear this notice and the full citation on the first page. Copyrights for components of this work owned by others than ACM must be honored. Abstracting with credit is permitted. To copy otherwise, or republish, to post on servers or to redistribute to lists, requires prior specific permission and/or a fee. Request permissions from permissions@acm.org.

e-Energy '19, June 25–28, 2019, Phoenix, AZ, USA

© 2019 Association for Computing Machinery.

ACM ISBN 978-1-4503-6671-7/19/06.

<https://doi.org/10.1145/3307772.3328293>

Future Energy Systems, June 25–28, 2019, Phoenix, AZ, USA. ACM, New York, NY, USA, 11 pages. <https://doi.org/10.1145/3307772.3328293>

1 INTRODUCTION

With all the innovation and developments like an increasing number of EVs and an increasing amount of renewable energy sources getting integrated into the grids' infrastructure, electrical grids are nowadays facing challenges they were just not designed for. Particularly, new requirements on low voltage distribution grids have to be fulfilled since the increase in EV penetration brings another set of problems in terms of Power Quality (PQ) and congestion in the different parts of the distribution grid [11, 23, 26]. The latter can lead to overheating of transformer windings, power-supply instability and accelerated degradation of line and transformer insulation, leading to premature equipment failure.

Heretofore, infrastructure dimensioning [19, 33] has been adopted by Distribution System Operators (DSO) as a guaranteed solution for those emerging requirements. That dimensioning has been based on worst-case conditions in all cases. Nevertheless, such a procedure is no longer attractive from an economic and technical point of view. State-of-the-art 22 kW charging power [25] by far exceeds the 4 kW estimate for a residential grid connection in central Europe. Consequently, more on-line monitoring and even active interventions during grid operation will be necessary to maintain critical boundary conditions such as line voltages and asset loading within safe limits.

Undoubtedly, guaranteed immediate and fast charging can only be realized with sufficient grid capacities at the connection point, in particular, required for public CSs. However, the variability and unpredictability of EV loads make that task hard and costly from the point of view of grid operators. As a result, a "smart approach" that makes use of available excess capacities of the grid elements can help to reduce grid connection costs, particularly, for the expected large number of private(semi) fast charging wall-boxes. Therefore, this paper proposes a solution for an active network operation at a low voltage level.

Inspired by the design of the Internet, which offers best effort services to elastic applications that back off in case of congestion, we design a controller based on the slow start algorithm of TCP congestion control. The authors of [5] introduce a comparison between a packet-switched communication network such as the Internet and the power distribution grid. According to their study, many concepts of the Internet have equivalents or good approximations in the power grid, namely, congestion, topology, sending measurements and controlling signals, self-protection and uncontrolled loads. The only main difference is the congestion notification. While the Internet has two types of congestion feedback: explicit and implicit, the

distribution grid has originally none of them. Precisely, the implicit mechanism is almost impossible¹ according to [5], whereas the explicit one does not exist in most of the distribution grids because of the lack of installed measurement devices. The trade-off between cost and leveraging is the reason behind that lack. However, such a notification mechanism in smart grids could provide information about the not only the congestion but also about other grid issues, i.e., power quality. Additionally, the lack of information in the low voltage grid is a major criteria design of this mechanism.

To achieve congestion avoidance on the Internet, TCP uses schemes such as *slow start* [20]. The mechanism is heavily influenced by "end-to-end argument" [10] whereby the congestion control is largely a function of Internet hosts. TCP maintains a *congestion window* ($Cwnd$) in order to limit the total number of unacknowledged packets that may be in transit end-to-end. In a similar way, grid operators use demand controlling to counteract some issues in the distribution grid, specifically, voltage drops and assets overloading. A demand controlling is has been mostly performed on relatively big loads such as EV. However, an important difference between the Internet and power network should be noted. A congestion in the network causes longer Round Trip Times (RTTs) because of increasing the packet queues at router. The Internets's TCP/IP uses RTT to autonomously detect the congestion. By using the statistics of the measured RTTs, a re-transmission timeout (RTO) is calculated on-the-fly. In contrary, the congestion in power grids is defined by events generated when some predefined threshold are crossed, e.g., voltage drop. Two factors determine the response time of any load controller: the arriving time of an event and the technical specifications of the controllable load, e.g., some EVs see the rapid changes in charging power as a sign of bad power quality, thus disconnect from CS. While the latter can be seen as a correspondence of flow control mechanism of TCP, the former depends on the delay coming from data gathering, data processing and consuming of event by the controller. As a result, the response time of a controller including the time of both notification and actuating is bounded by the technical constraints of both the charging power adaptation by the car and the power grid. By analyzing the process chain for measuring, analysis and decision making (end-to-end delay), that delay is usually upper bounded by the frequency adaptation of charging power by the car, thus we designed the smart charger to react periodically based on all arrived events (notifications) in that time horizon. Nevertheless, the SC can react differently in terms of quickness based on the degree of importance of the arriving event. The response time can be adjusted dynamically in a similar way to the RTO.

Based on the similarity of the congestion problem in TCP and the demand controlling in the distribution grid discussed in the previous paragraph and in [6, 24, 36], we develop an EV smart charger inspired by the slow start. It uses a discrete charging rate similar to the $Cwnd$ in TCP. Thanks to a notification mechanism proposed in [4], the smart controller can react to different events in the distribution grid by increasing or decreasing the charging power similar to the TCP slow start. The notification mechanism is distributed and it adopts a traffic light model [7] in order to design an EV

charging controller like TCP slow start. A component running at each connection point of a CS generates indication signals using selected data from certain Measurement Points (MP) distributed through the grid. The aforementioned component generates those indications using a hierarchical logic considering the loading of grid assets and the local voltage at the CS or at another point in the grid considered as critical in terms of voltage.

The remainder of this paper is structured as follows: In Section 2 we discuss related work. The architecture is described in Section 3, after that, we introduce the designed controller in detail in Section 4. The results of different scenarios using a pure (co-)simulation are presented in Section 5. Finally, we highlight future work and conclude the paper in Section 6.

2 RELATED WORK

Potential impacts of introducing a large number of EVs to the power distribution network have been studied extensively in the literature and many ideas have been introduced to use the EV penetration for supporting the grid.

The solutions are very diverse and can fall under two main categories in terms of functionality: charging scheduling [17, 18, 30] and charging control [3, 4, 6, 8, 21, 22, 29]. However, there are three types of charging control depending on where the charging decision takes place:

- (1) Centralized [8, 21]: An EV aggregator is responsible to take an optimal charging decision for all the connected EVs.
- (2) Decentralized [3, 22, 29]: The whole computation is done by the local entities, i.e., no entity tells any other entity what to do. The decision is completely independent.
- (3) Distributed [4, 6]: Here is still a presence of EV aggregator, e.g., hierarchical or central unit, which does part of the computation and forwards the output to local controllers. A local controller reacts based on the forwarded and other local information.

One one hand, a coordinated control at different levels of a hierarchical distributed system such as the power grid becomes infeasible with a centralized control as discussed in a white paper [34]. On the other hand, decentralized approaches either depend only on local grid data at the CS or assume all the required grid data is available locally at the controller. Those approaches ignore the fact of lacking data from the distribution grids. Furthermore, the EV charging ecosystem contains multiple actors who prefer to share information as little as possible about their assets, specifically the DSO about the low voltage grid. Therefore, distributed approaches are the best solutions in order to keep the communication among the actors as low as possible and to separate the different concerns of ecosystem actors.

Based on the discussion in the previous paragraph, a notification mechanism managed by the DSO according to the individual properties of each distribution grid is designed. Using this mechanism, the DSO can hide many details from the controller by sending only a single value describing the grid state; see Section 3.3. In contrast to the mechanism proposed in [6], which requires a heavy and synchronous communication overhead and only considers the congestion in distribution grids, the used mechanism considers both congestion and voltage control. While the authors of [6] chose to

¹Sensing the voltage and frequency locally at end nodes can reveal some information about the grid [16]

solve an optimization problem at the controller to ensure that network resources are used efficiently and each EV charger receives a fair share, we adopted the TCP slow start algorithm. The simplicity, the similarity as described in Section 4.1 and the prioritization of power quality are the reasons behind that choice.

In contrast to other existing work, the proposed controller considers both voltage and overloading of assets. It allows more energy to be charged into the EV battery without violating the predetermined operating conditions of the grid. Thanks to the notification mechanism, the communication overhead has been reduced. We make three specific contributions:

- A notification mechanism as a part of a smart charging architecture proposed in [4].
- Designing and evaluating a TCP-like charging controller as a part of the smart architecture.
- A comparison scenario between solutions based On Load Tap Changer (OLTC) and smart charging in terms of voltage control.

3 DISTRIBUTED SMART CHARGING ARCHITECTURE

For the sake of clarity, an architecture proposed in a [4] is described in this section since the proposed controller in this work is a part of that architecture.

3.1 The Vision

We envision a system in which a public CS can react immediately to different events happening in a distribution grid in terms of overloading the assets and the degradation of power quality, namely, voltage drops on the feeder line. The reactions of each individual CS are independent of other CSs and based only on the current state of the grid² regardless of the reactions of the other existing CSs in the system.

An event-driven engine (e.g., Apache Kafka [15]) handles the events that are triggered by MPs based on real-time data [31]. The MPs are distributed through the grid at certain places. The locations and the data resolution of each MP are determined by the DSO. The status of the grid in terms of power quality and congestion is described by a set of Key Performance Indicator (KPI)³ classes, e.g., voltage and current. Some of those KPIs are directly measured by a MP and others can be derived from the measured values, e.g., the loading percentage of an asset. Thanks to the efficient communication and control infrastructure, a smart charger can react nearly immediately or at a certain rate to the triggered events, averting the use of grid protection actions such as circuit breakers.

Based on the triggered events and thresholds of the KPI classes as predefined by the DSO, the system can indicate the status of the grid as optimal, degraded and critical. Hence, actions are initiated by controlling unit (i.e. PQ-Indicator and Smart Charger) in order to keep the considered KPI within the allowed boundaries and satisfy the required charging energy predetermined through a predefined charging profile by the end user. The proposed vision is similar to the one used on the Internet to control elastic flows (e.g., fast TCP).

²In this work and as a part of the proposed TCP-like controller, a number of previous grid states are taken into consideration.

³The definition of KPI in the paper does not conform to the typical definition of KPI

Whereas on the Internet, there are different events such as arriving, lost and double acknowledgments to control the transmission rate of the hosts, the proposed system creates similar events to increase or decrease charging rate of an active charger in order to give a hand for stabilizing the grid and enhancing the power quality.

On one hand, the proposed system is designed in order to tackle the congestion of one asset in the grid; namely the transformer. The transformer is said to be congested when the total measured apparent power of the transformer is higher than a predefined threshold wherein an event is triggered. On the other hand, we pay attention for keeping the voltage in a predefined range by the DSO since voltage limitation in a node is one of many system conditions (e.g. transient stability, dynamic stability, reliability) of the distribution network which contribute to congestion of the network. The end nodes (controllable loads) are notified about all the events of violating the thresholds of both transformer and voltage by a hierarchical mechanism described in Section 3.3. The proposed controller receives signals and reacts in a way to keep the voltage and the transformer load in the optimal range limited by the thresholds.

While the proposed controller in this work mimics the TCP slow start mechanism to control the used power capacity of the EV charger, the proposed controller in [4] uses a Finite-State-Machine (FSM) to present the different states of the system, namely, optimal, degraded, critical, standby and unplugged EV. Three kind of events that can trigger the state transition are considered: Input of a new PQ-Indic, unplugging of EV and changing of the State of Charge (SoC) of the battery. FSM-based controller takes into account only the current state of the grid to determine the correct power allocation at the CS. Our controller considers the previous states of the grid in order to recognize the different events in the grid.

The system does not require us to predict SoC or the EVs mobility. In that regard, the connection point of the CS is considered instead of a single connector. The CS is able to contribute to any events of the grid as long as one charging connector is active. The total demand of the CS (aggregated of all connectors) can be controlled every few minutes. The coordination of the available capacity at the connection point is not a part of this paper; nevertheless, a fair or proportional distribution can be used. As a result, a quick response to changes in the distribution grid due to fluctuations in uncontrolled loads is possible since neither prediction models of EV arriving rate nor charging behavioral of the end users is required.

The proposed vision can be formulated as an optimization problem. Its objective function is defined with a goal of maximizing the used active power at each CS. The problem is subjected to three kind of conditions: (1) the transformer load is smaller than a predefined threshold, (2) the voltage at the CS, transformer and the critical point is in a certain range, (3) the typical equations of the power flow. Furthermore, a further condition can be added to ensure fairness among the active CSs. However, the problem is nearly similar to the problem of calculating an Optimal Power Flow (OPF) but it should be solved in a very short time since it is intended to react in real-time, e.g., every one minute. The proposed problem presents an increased computational complexity which is mainly caused by two factors. The first corresponds to the inherent network non-linearities. The second is the size of low voltage networks. As a consequence, conventional optimization approaches are inadequate

because of the local minimum solutions. On the contrary, heuristic or meta-heuristic techniques are considerably time-consuming and cannot be applied in real-field conditions [28]. However, solving such a problem by a centralized entity can provide proof about the con(di)vergence of the proposed system. We defer the formulation and solving of this problem to the future work as it is not a part of this work and needs a lot of discussions.

3.2 Measurements and Event-driven Architecture

The distribution power network is assumed to be equipped with MPs installed at the critical points in the grid such as transformer and CSs. The low voltage grid has typically not been equipped with MPs to monitor every point in the grid⁴. The trade-off between cost and leveraging is the reason behind that. Those MPs are configured to collect the KPI values in real-time. The data stream is in high resolution to allow the indication of the different power quality issues in the grid. Eventually, a generic and fault tolerant data processing architecture is required to handle such big data stream. Furthermore, the measured KPI values are most interesting when they are beyond a certain threshold, e.g., the voltage is greater or lower than $\pm 10\%$ of the nominal voltage. These events are triggered by MP due to unusual KPI values and sent to an event-driven streaming service using Power Line Communication (PLC) or dedicated Internet access. Only the events that can be handled by the CS through setting the correct configured parameters are subscribed to the responsible controlling component.

Apache Kafka is a well-known distributed streaming platform that provides a scalable and resilient event store. It is used to build reliable and real-time data pipelines to transfer data between systems or applications. The events are stored in topics for which multiple producers and consumers may exist. However, to enable efficient real-time processing of these infinite data streams, the reactive streams [2] initiative comes into play, e.g, Akka streams [1]. It provides a standard for asynchronous stream processing, with non-blocking back pressure. This means that the consumer(s) should not be overwhelmed by the producer(s); thus letting the streaming solution implement and control bounded queuing.

However, the size of each sent event is not that big; it equals $104 + 17n$ bytes, where n is the number of measured KPIs. The embedded data in the event includes two Universally Unique Identifier (UUID) for the MP and its location, timestamp and Kafka header. hence, an LTE connection for each MP with an approximate volume of one GB would be enough.

3.3 Real-time Indication of the Status of a Distribution Grid

The indication mechanism used in this paper and proposed in [4] complies with four design criteria. First, excessive intelligence unnecessarily complicates the system. Second, it assigns a high value to the local conditions over the remote ones⁵. The locally concentrated impact of DG and uncontrolled loads provides further

⁴With the roll out of the smart meters, the situation may change

⁵In [16], it has been shown that local sensing of the line voltage or frequency at end nodes can be used to implicitly infer the aggregate demand or the power imbalance at higher levels in the distribution network.

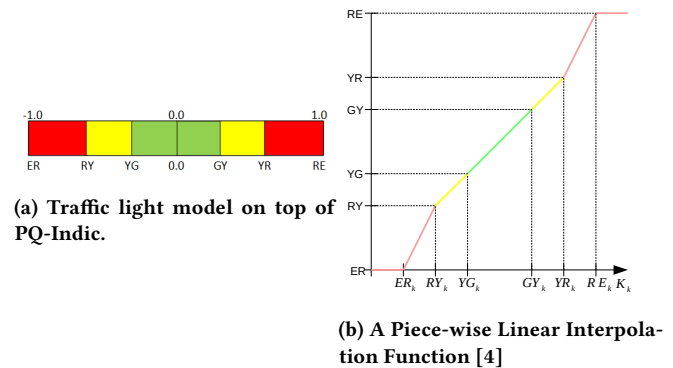


Figure 1: Traffic light Model

evidence in this respect⁶. Third, it takes into account that the connection points in the grid are not on the same degree of importance, e.g., the transformer is extremely important in the low voltage grid as a single point of failure. Fourth, apart from the location of the raising PQ issue, the grid status cannot be seen only as good or bad, rather coarse-grained indication is possible. In other words, the DSO considers some operating conditions in the grid as not optimal but sees no need for applying contingency measures. Thus, a very smooth change in the behavior of the controllable loads in the grid can move back into the optimal (normal) operating conditions.

Based on the previous discussion, a distributed notifications mechanism about the grid status is developed. A component called "PQ-Indicator" runs at the connection point of each CS and indicates three grid states: good, not optimal, and critical. Those states can be defined over the allowed ranges of different KPIs of the distribution grid. Thus, the concept of a traffic light model is applied to describe the status of the grid in terms of a predefined KPI as follows:

- Red Phase: Represents a critical situation in the grid. A relative drastic action (e.g., increase/decrease of the CS demand) has to be taken by each active SC in order to mitigate the stress on the grid.
- Yellow Phase: Represents a warning phase. The situation is not critical but still cannot be considered as optimal. A smooth action of the SC can be enough to move back into the stable status.
- Green Phase: Represents a stable phase, thus, no need for any further SC reactions concerning the grid.

The output of *PQ-Indicator* is a normalized value $PQ-Indic \in [-1, +1]$. The colors are defined on top of *PQ-Indic* as depicted in Figure 1a. While the negative value of *PQ-Indic* means a reduction in CS demand is required, the positive one refers to a required increase. As a result, two kind of red signal are existing (R^+ , R^-) and yellow signal as well (Y^+ , Y^-).

In that regard, the six thresholds, ER_k , RY_k , YG_k , GY_k , YR_k , RE_k , for the red, yellow and green areas are defined for each KPI class k separately. The values of k are translated according to a piece-wise linear interpolation function (Figure 1b) to a value $PQ-Indic_k$. The piece-wise nature is the reason behind that choice. It is simple, preserves order and allows weighting and shifting of the range of individual KPI classes.

⁶This conclusion is a direct result of applying Ohm's law.

Afterward, the different $PQ-Indic_k$ are combined using two criteria A_1 (overloading an element of the grid) and A_2 (voltage level). However, current used CSs have only the capability to mitigate overloading and voltage level by limiting the charging power. Nevertheless, this list may be extended to include additional criteria such as harmonics and frequency deviation.

While the focus of this work is only on the transformer for A_1 , three points are considered for A_2 , namely, the transformer, the CS and a critical point predetermined by the DSO. Those criteria are ordered according to their importance in terms of grid stability.

3.4 Smart Charging Control

The smart charging algorithm starts once a vehicle is plugged into a connector. It uses real-time indications of the PQ-Indicator as a single input about the grid. Additionally, it considers the energy requirements of the end user. Thanks to the concept of charging profile introduced by OCPP 2.0 [27]⁷, our smart charging algorithm controls the charging process in reality by defining external profiles at a high stack level.

According to OCPP 2.0, CSs can handle different types of charging profiles: ChargingStationMaxProfile, TxProfiles, and ChargingStationExternalConstraints. Those different profiles are stacked and used by their prioritized stack level. The Composite Schedule combines the different profile types by calculating the minimum in each time interval.

Furthermore, an experiment using Power Hardware in the loop (PHIL) is stated in [4]. It shows the response of the EV emulator and the real EV to the charging signal via IEC 62196. This standard supports a Pulse Width Modulation (PWM) current signal, which indicates the amount of current that can be provided by the CS.

4 TCP-LIKE SMART CHARGER

Because of the similarity of the problem in hand with the network congestion of the Internet, we decide to adapt the TCP-Reno slow start mechanism to implement the smart charging controller described in Section 3.4. While on the Internet we have an implicit notification mechanism based on receiving or losing acknowledgment of the sent data packet, we use a PQ-oriented mechanism described in Section 3.3.

In TCP slow start, there are multiple events: Time out, crossing the thresholds ($THOLD_{ss}$), and duplicate ACK. Each of those events requires accordingly different approaches to deal with in terms of congestion: Initialization (Init.), Slow Start (SS), Congestion Avoidance (CA), and Fast Re-transmit and Recovery (FRR). Table 1 depicts a comparison between the TCP slow start and EV SC.

4.1 TCP Slow Start vs. Smart EV Charger

In this section, we elaborate on the information stated in Table 1.

How is the network status perceived?

- **In TCP:** TCP perceives congestion on an end-to-end feedback basis between sender and receiver, by looking out for acknowledgments received after the packets are sent. Both

the number and content of the acknowledgments are an indication of the status of the network.

- **In SC:** The status of the distribution grid is indicated based on certain predetermined KPI thresholds by the PQ-Indicator. Here, the indication mechanism is explicit and based on measurement data.

How to control the sending rate/charging power?

- **In TCP:** By scaling of $Cwnd$. The basic idea is when the sender learns about the status of the network, it triggers an action to slow down/speed up the sending rate of packets.
- **In SC:** With changing the charging power allocated to the CS. When SC learns about a critical/warning status in the distribution system, it reduces/increases the currently used charging power of the corresponding CS.

What are the events that trigger actions?

- **In TCP:** While receiving an ACK in time means no congestion in the network, timeout indicates the loss of packet or ACK, mostly due to congestion in the network. Otherwise, receiving duplicate ACKs indicates a situation where the packets are being delivered out of order that implies the loss of one or more packets in transit.
- **In SC:** For detecting events, our SC looks out for $PQ-Indic$; the output of PQ-Indicator. In case $PQ-Indic \in G$ (green), it is considered as no issues in the grid. Otherwise, if $PQ-Indic \in R^-$ (negative red) it is similar to the timeout event of TCP. Finally, $PQ-Indic \in Y^-$ (negative yellow) indicates a warning, similar to duplicate acknowledgments in the slow start. However, $PQ-Indic \in R^+ \cup Y^+$ is considered as changing the maximum limit of possible charging capacity. More details are presented in Section 4.2

How are the SS and CA phases distinguished?

- **In TCP:** There is a threshold $THOLD_{ss}$, until this threshold an exponential increase of $Cwnd$ is taken place (SS phase) and above which a linear increase is applied (CA phase).
- **In SC:** Similar to TCP, we have a threshold value up to which the power increase is quick. We consider an additional exponential increase so that the allocated power at CS increases exponentially using a predefined constant ϵ called a change-rate. Above the threshold, the power increase turns linear w.r.t. the same constant ϵ .

Aspect	Slow Start	EV Charging
Events	Timeout, ACKs, $THOLD_{ss}$	Color signal
Status perceived	Based on ACKs received	KPI Thresholds
Participants	Sender, Internet (Receiver)	CS, Distribution grid
Control parameter	Sending rate	Charging Power
State	FRR, CA, SS	Critical, Warning, Good

Table 1: TCP slow start vs. Smart EV Charging

4.2 Methodology

In this section, the used capacity of an active charging process at charging station C_i at time t is denoted as $\mathcal{U}_i(t)$. The maximum physical capacity of C_i is written as \mathcal{M}_i and the user's charging profile is denoted as $C_i(t)$. In all cases, $\mathcal{U}_i(t)$ should not be bigger than \mathcal{M}_i . Furthermore, the minimum charging power needs to be

⁷Open Charge Point Protocol (OCPP) has been developed by several parties to enable cross-manufacturer communications with charging infrastructure. It is widely used and supported by most CSs in the market.

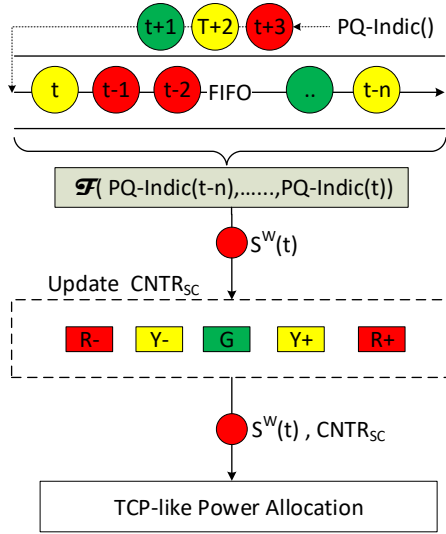


Figure 2: TCP-like Smart Charger

set to a value C_{min} higher than zero to avoid disconnection of the vehicle. A safety upper margin is defined by $\mu < 1$ in order to stay aligned with the users charging profile regarding the battery state of health and the charging duration. This safety margin is used as a buffer to compensate grid problems that may lead to a short reduction of charging power. Additionally, we defined a limit β where $\mu < \beta < 1$ to distinguish between the warning and critical increase required in the power grid, i.e., the case of $PQ-Indic \in R^+ \cup Y^+$. Hence, we have three limits max_G , max_{Y^+} , and max_{R^+} for each increasing signal G , Y^+ , and R^+ respectively. The limits are defined as follows:

$$\begin{aligned} max_G &= (1 + \mu)C_i(t) \\ max_{Y^+} &= (1 + \beta)C_i(t) \\ max_{R^+} &= M_i \end{aligned} \quad (1)$$

Similar to TCP, we maintain a threshold $THOLD_{ss}$ that defines the point where SS phase stops and the CA phase begins.

The logic of the SC contains three steps as depicted in Figure 2. In the first step, the SC estimates the most dominating states of the grid $S^W(t)$ in the last seconds. That estimation is based on a predefined-size set of previous indications of grid states, namely, $PQ-Indic(t)$. The importance of this step raises in the case of the difference between the frequency of performing the state indication and the reaction of the SC. Usually, the grid indication is done in a higher frequency than the SC reaction in the purpose of accuracy. For example, the indication is done every 15 seconds and the SC react every minute. Next, the SC distinguishes among the different events in a similar way to the TCP slow start as described in Section 4.1 through setting a set of counters $CNTR_{SC}$ for each color signals. Finally, the SC allocates the suitable amount of power based on the correct reaction for each considered state like the slow start algorithm. The aforementioned steps are described in details below.

(1) **Calculating a weighted average indicator of the grid status $S^W(t)$**

To this end, the SC maintains a First-In-First-Out (FIFO) queue called LastValuesStore (LVS) to store the last n values of $PQ-Indic$; $[t - n, ..t]$. The queue is updated by each new arrival of $PQ-Indic$ value at the SC. By each SC step,

a weighted average of the existing values in the queue is calculated. The output refers to a weighted average indicator of grid status at time t ($S^W(t)$).

Equation (2) depicts how the weighted average indicator is calculated, where ω_k is a list of the same size as LVS and contains weights for each index of LVS (k). ω_k is defined in such a way that the most recent $PQ-Indic$ values are given higher weights thus more importance compared to the earlier values.

$$S^W(t) = \frac{\sum_{k=t-n}^t LVS_k \cdot \omega_k}{\sum_{k=t-n}^t \omega_k} \quad (2)$$

(2) **Updating the SC counters $CNTR_{SC}$**

The SC maintains a counters array $CNTR_{SC}$, which holds counters for each of the operational phases based on the traffic light model. The counters $CNTR_{R^-}$, $CNTR_{Y^-}$, $CNTR_G$, $CNTR_{Y^+}$, and $CNTR_{R^+}$ keep in track the number of consecutive occurrences of the phases R^- , Y^- , G , Y^+ , and R^+ respectively. The values saved in $CNTR_{SC}$ are important in order to determine the action that needs to be taken in the next step. Initially, each counter is initialized to zero. For simplification purposes, we use the symbol $S(t)$ instead of $S^W(t)$ in order to refer to the current grid operational phases calculated in step 1.

During each SC step and based on the value of $S(t)$, the corresponding counter $CNTR_{S(t)}$ is incremented by one. Additionally, a change in $CNTR_G$ is performed depending on the updated value of $CNTR_{S(t)}$. The reason for this additional change is an added importance for the green status, as it plays a role in the exponential growth of the charging power during the SS phase in Algorithm 1. Whereas the number of corrected received acknowledgments in each step determines implicitly the exponential growth of $Cwnd$ in TCP slow start, an accumulator is required in our approach since the indication of the grid status is done in each step by a single value $S(t)$. Hence, we increment or keep $CNTR_G$ unmodified for the phases that indicate an increase in charging power, namely, G , Y^+ , and R^+ . Equation 3 depicts how $CNTR_G$ is used to calculate the exponential value on change-rate ϵ during SS phase of Algorithm 1.

$$\begin{aligned} \mathcal{U}_i(t+1) &= \mathcal{U}_i(t) + \epsilon^{CNTR_G} & \mathcal{U}_i(t) < THOLD_{ss} \\ \mathcal{U}_i(t+1) &= \mathcal{U}_i(t) + \epsilon & \mathcal{U}_i(t) \geq THOLD_{ss} \end{aligned} \quad (3)$$

Thus for every $S(t) \neq G$, all counters $CNTR_{SC}$ except $CNTR_{S(t)}$ are set to zero since the consecutive occurrence of an event is significant rather than each individual event (similar to the TCP slow start). Eventually, $CNTR_G$ and $CNTR_{S(t)}$ are updated as follows:

- $S(t) \in R^+$: We increment both $CNTR_{R^+}$ and $CNTR_G$ by one.
- $S(t) \in Y^+$: We increment $CNTR_{Y^+}$ by one. If updated $CNTR_{Y^+}$ is one, $CNTR_G$ does not change. Otherwise, we increment $CNTR_G$ by one.
- $S(t) \in R^-$: We increment the $CNTR_{R^-}$ by 1. If updated $CNTR_{R^-}$ is one and the previous phase is green then $CNTR_G$ is decremented. In all other cases, $CNTR_G$ will be set to zero.

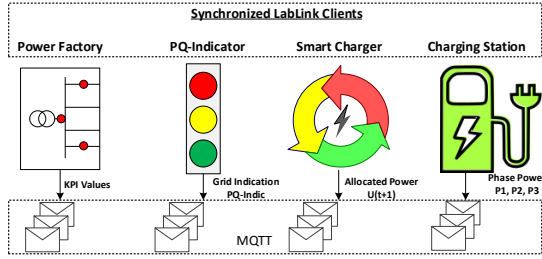


Figure 3: Evaluation Setup

- $S(t) \in Y^-$: We increment $CNTR_{Y^-}$ by one. If updated $CNTR_{Y^-}$ is one, $CNTR_G$ does not change since it can be a transit status. If $CNTR_{Y^-} = 2$ we decrement $CNTR_G$ by 1, Otherwise, $CNTR_G$ is made zero.
 - $S(t) \in G$: We increment the $CNTR_G$ by one. However, the first green signal causes a decrement of one in any other counter if its value is not already zero. This is under the precautionary measure assuming the first green might be a transitory phase and the situation might return to unstable phases. Otherwise, we set other four counters to zero.
- (3) **TCP-like allocating of the charging power**

Based on the output of the previous two steps: $CNTR_{SC}$ and $S(t)$, appropriate action is taken in order to determine the charging power $\mathcal{U}_i(t+1)$ in the next time step. The algorithm should start slowly by setting $\mathcal{U}_i(0)$ equal to C_{min} since a conservative approach concerning the grid stability is adapted. The initial value of $THOLD_{SS}$ is set to a portion α of the predefined user's charging profile in each time slot t ; $THOLD_{SS} = \alpha \cdot C_i(t)$.

Algorithm 1 depicts how SC adjusts the active power and the threshold based on the value of $S(t)$. However, the algorithm does not conform completely with the TCP slow start algorithm since there is no perfect match between the Internet and the studied system, namely, the power grid. In addition to the changing of max limits clarified at the beginning of this section using Equation (1), we avoid making drastic changes similar to the slow start by setting the values of $THOLD_{SS}$ and $\mathcal{U}_i(t)$ since such a change can lead to either ping-pong effect or negative impact in terms of voltage drop. Precisely, neither $THOLD_{SS}$ nor $\mathcal{U}_i(t)$ is set to zero through timeout event for example. Otherwise, this action is configured based on the nature of each individual charging process. For that, three additional parameters are defined: λ_1 , λ_2 , and λ_3 ; where $0 \leq \lambda_3 \leq \lambda_2 \leq \lambda_1 \leq 1$.

Finally, the case of $S(t) \in Y^+ \cup R^+$ is not described in details in Algorithm 1 and merged with the case of the green status⁸. However, similar to the first Y^- , we ignore the first Y^+ and change the maximum limit regarding Equation 1 from the second consecutive Y^+ . While the first R^+ equals to two consecutive Y^+ , two or more consecutive R^+ adjust the maximum limit to be max_{R^+} .

Algorithm 1 TCP-like Charging Power Allocation

```

Require:  $S(t)$ ,  $CNTR_{SC}$ ,  $C_i(t)$ ,  $THOLD_{SS}$ 
Ensure:  $C_{min} \leq \mathcal{U}_i(t) \leq M_i$ 
switch ( $S(t)$ )
case  $R^-$ :
  if  $CNTR_{R^-} = 1$  then
    // Duplicate acknowledgments
     $THOLD_{SS} = \lambda_1 * \mathcal{U}_i(t)$ 
     $\mathcal{U}_i(t+1) = THOLD_{SS}$ 
  else if  $CNTR_{R^-} > 1$  then
    // Time Out
     $THOLD_{SS} = \lambda_2 * \mathcal{U}_i(t)$ 
     $\mathcal{U}_i(t+1) = \lambda_3 * \mathcal{U}_i(t)$ 
  end if
   $\mathcal{U}_i(t+1) = \max(\mathcal{U}_i(t+1), C_{min})$ 
case  $Y^-$ :
  if  $CNTR_{Y^-} = 1$  then
    // Warning: no change
     $\mathcal{U}_i(t+1) = \mathcal{U}_i(t)$ 
  else if  $CNTR_{Y^-} > 1$  then
    // Duplicate acknowledgments
     $THOLD_{SS} = \lambda_1 * \mathcal{U}_i(t)$ 
     $\mathcal{U}_i(t+1) = THOLD_{SS}$ 
  end if
   $\mathcal{U}_i(t+1) = \max(\mathcal{U}_i(t+1), C_{min})$ 
case  $G, Y^+, R^+$ :
  Calculating MAX based on Equation 1
  if  $\mathcal{U}_i(t) < THOLD_{SS}$  then
    // Slow start stage
     $\mathcal{U}_i(t+1) = \mathcal{U}_i(t) + \epsilon^{CNTR_G}$ 
  else
    // Congestion avoidance stage
     $\mathcal{U}_i(t+1) = \mathcal{U}_i(t) + \epsilon$ 
  end if
   $\mathcal{U}_i(t+1) = \min(\mathcal{U}_i(t+1), MAX)$ 
default:
  End phase: SoC= 100%,  $\mathcal{U}_i(t+1) = 0$ 
end switch

```

5 EVALUATION

The objective of this section is to evaluate the impact of the TCP-like SC on the grid in terms of power quality and overloading the transformer. Furthermore, a comparison between the proposed SC and a FSM-based SC proposed in [4] is introduced. Both SCs use the output of the PQ-indicator as an indication about the current grid status. While the FSM-based SC takes into account only the current status of the grid to determine the correct power allocation at the CS, the TCP-like SC considers the previous states of the grid in order to recognize the described events in Table 1. Finally, we propose a scenario where a solution using the OLTC transformer instead of the SCs is used. We compare it with our solution and discuss the advantages and disadvantages.

5.1 Setup

For all the following evaluation scenarios, the co-simulation framework *AIT Lablink* is used [14]. However, the required components (described in Section 3) for testing the proposed SC are implemented as LabLink clients as depicted in Figure 3. Lablink supports communication among those clients using publish/subscribe concept facilitated by *Message Queuing Telemetry Transport (MQTT)* message bus. Here, the PQ-Indicator subscribes for the KPI values from different MPs in the grid and publishes the calculated grid indications that are subscribed by the SC. The CS subscribes for the charging signals of the SC for further changes in its charging process. The CS client allocates the power equally on the three phases. Apart from that, the allocation can be in a way supporting the phase imbalance that is not a part of this paper. Lablink supports central simulation manager *Synchost* that provides sync. service to initialize, synchronize and control of the simulation flow configuration centrally among the Lablink clients [32].

⁸Because of the page limit

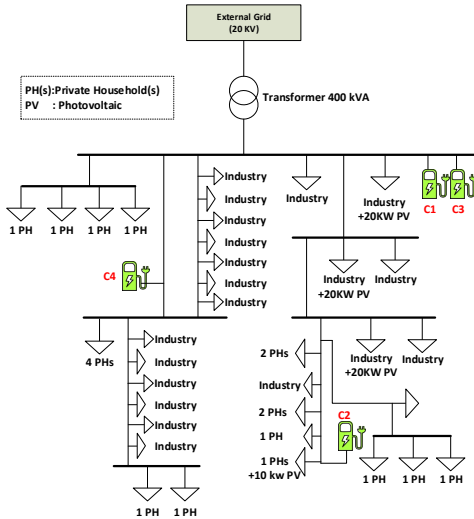


Figure 4: Placements of Four CSs in the Tested Grid.

The smart charging algorithm is tested against a simulated version of a low-voltage distribution network located in a small city in Germany; a schematic illustration is stated in Figure 4. The used grid is similar to the used one in [4], with 64 cables connecting 22 households, 21 industrial loads, 3 photovoltaic (PV) systems and four connected charging stations. The maximum distance to the transformer is given by a cable with a length of 485 meters. DIgSILENT PowerFactory [12] is the grid simulation tool used and is one of the LabLink clients. Four charging stations (C_i) are placed at different points in the grid as depicted in Figure 4. One CS is located as far as possible from the transformer at the critical point of the grid in terms of voltage drop (C2). The second CS is located at the second main feeder line that is supplied by the transformer (C4) and the remaining two CSs are located near to the transformer, as it is the case in the real grid.

Three kinds of 24-hour profiles are fed into the simulation: realistic household load profiles [35], BDEW⁹ load profiles for industries, and real generation profiles for the PV systems.

	ER	RY	YG	GY	YR	ER
Load (kVA)	400	300	150	0	0	0
Voltage (V)	220.94	222.94	223.94	233.94	238.94	240.94

Table 2: Thresholds of the KPI Classes: Overloading and Voltage Level.

C_{min}	$C_i(t)$	M_i	α	μ	β	ϵ	λ_1	λ_2	λ_3
1.3kW	22kW	30kW	0.6	0.1	0.25	2.0	0.75	0.5	0.25

Table 3: Parameter configurations of TCP-like SC

The KPI thresholds for voltage and loading of the transformer are configured in the PQ-Indicator as shown in Table 2. From EN 50160, we know that in low and medium voltage networks the voltage level must be within $\pm 10\%$ of the nominal voltage during 95% of the week measured by 10 minutes mean RMS values [13].

⁹Bundesverband der Energie- und Wasserwirtschaft e.V

As the maximum allowed voltage deviation includes the medium voltage network is constantly transmitted to the low voltage grid in case no OLTC is installed, we decided to use a smaller range of $\pm 3\%$ and a time interval of one minute. Due to the setup of our test grid, overloading of the transformer starts at 37.5% of the rated apparent power of the transformer, which is given by 400kVA.

The simulation period is 24 hours with load and PV generation data of a real grid. The parameters used in the smart charging algorithm are shown in Table 3. C_{min} is 1.3 kW, the minimum charging power provided by the SC to the charging station in order to stay connected. For our test, we use a constant user charging profile of 22 kW for each C_i . Furthermore, the maximum power that can be provided by the SC is set to 30 kW, which is assumed also to be the maximum physical limit of all CSs M_i . The change-rate constant (ϵ) value is taken for the test is 2, note that this value should not be less than 2, since doing so would beat the basic idea of control actions in Algorithm 1 which is having power increase higher during SS phase than CA one. The remaining parameters are chosen in a way that is best suited for the smooth transition of the charging control signal and its effect on the grid.

5.2 Analysis

We consider three scenarios for evaluating the impact of the algorithm on the grid power quality. First, the best-case scenario, where no CS is connected to the grid during the simulation period implying no considerable power quality issues in the grid. Second, the worst case scenario, where all four CSs are connected to the grid and are charging continuously with a constant charging profile $C_i(t)$ throughout the whole simulation period, i.e., uncontrolled charging implying high-risk power quality issues in the grid. Hence, we can cover more use cases in terms of raising issues in the grid. The third scenario is our SC scenario having controlled charging at all four CSs. The first two scenarios form the baseline, $Baseline_{Min}$, and $Baseline_{Max}$ accordingly. Finally, the results of the proposed smart charging algorithm are compared to the results of the FSM-based SC. To this end, the same parameters configuration proposed in [4] are used.

This section aims to answer the following questions regarding the results obtained by simulation in the tested grid:

- (Q1) How does the SC algorithm improve the voltage level at the critical node of the grid?
- (Q2) To what extent is the overloading of the transformer avoided in order to maintain power quality?
- (Q3) How do our results improve the power quality when compared to the FSM-based SC?
- (Q4) What is better, OLTC-based solution or SC-based solution?

The initial analysis of the results shows that the period between roughly 8:00 - 12:00 and 16:00 - 20:00 are peak hours in a day where the load in the grid is high. It is resulting in a voltage drop greater than 3% and overloading at the transformer even during the $Baseline_{Min}$ scenario. During this time, SC restrains from further adding the CS load to the grid by reducing the charging power at CS to a minimum value (C_{min}). Thus, avoiding further strain on the situation of the grid. As the algorithm assumes only one direction charging, i.e., Grid-to-Vehicle (G2V), the degraded power quality during the peak hours cannot be compensated by the SC.

Design of a TCP-like Smart Charging Controller

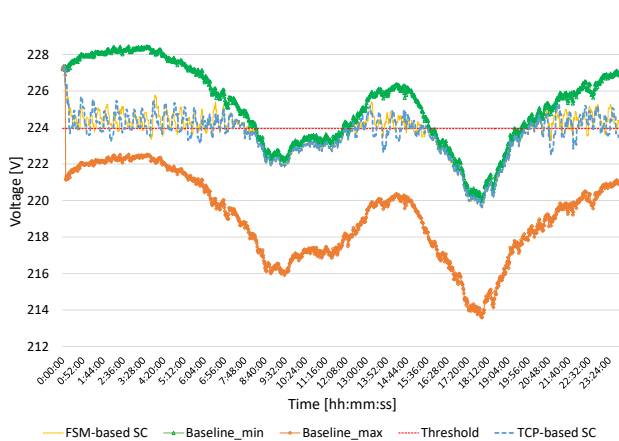


Figure 5: Voltage level at the Critical Node.

The following three sections focus on explaining the results from TCP-like SC during off-peak hours in detail.

5.2.1 Voltage level at the critical node. First, comparing the voltage level at the critical node in SC scenario to the baseline scenarios is depicted in Figure 5. In that figure, triangles and rhombuses show the voltage level during the two baseline scenarios. Furthermore, the results of using the SC as a control mechanism at each CS are represented by the dashed blue and solid saffron lines; TCP-like SC and FSM-based SC respectively. As seen in the graph, the algorithm controls the CS such that the voltage level is mostly above the threshold line and falls mostly within 1V below the threshold limit by crossing. In the worst case, the voltage drops to 222.4V during the whole day. The SC rectifies the voltage drop below the threshold value by reducing the power allocation at the CS in the next step. In the $Baseline_{Min}$ scenario, the voltage level during off-peak hours is well above the threshold and drops to a critical level during the $Baseline_{Max}$, precisely, 213.5V. Furthermore, the magnitudes of the voltage drop spikes are higher by TCP-like SC in compare to the ones of FSM-based SC. The reasons behinds that is the fast increasing actions taken by the TCP-like SC in the slow start stage. For example, the period between 12:00 AM and 6.30 AM, the PQ-Indicator indicates a stable situation at the grid, hence algorithm performs normal SS exponential increase which can cause sudden voltage drop during fast increasing of the load at certain points of time.

Finally, the number of times when the voltage level crosses the threshold with TCP-like SC is 11% more than that of FSM-based SC. In the worst case, the voltage drops to 223.2V by FSM-based SC in comparison to 222.4V by the TCP-like SC. The voltage control achieved when using FSM-based SC is comparatively better than that of TCP-like SC.

5.2.2 Overloading the transformer. Second KPI class we consider for evaluating our SC is the loading of the transformer in terms of the total apparent power (S). As depicted in Figure 6, during $Baseline_{Max}$ scenario the transformer crosses the threshold for 72.2% of the day. While FSM-based SC reduces this value to around 5%, our TCP-like SC reduces the value to 1.3% of the day. Furthermore, the total energy crossing the threshold is 27% higher in the scenario of the FSM-based SC in comparison to the scenario

e-Energy '19, June 25–28, 2019, Phoenix, AZ, USA

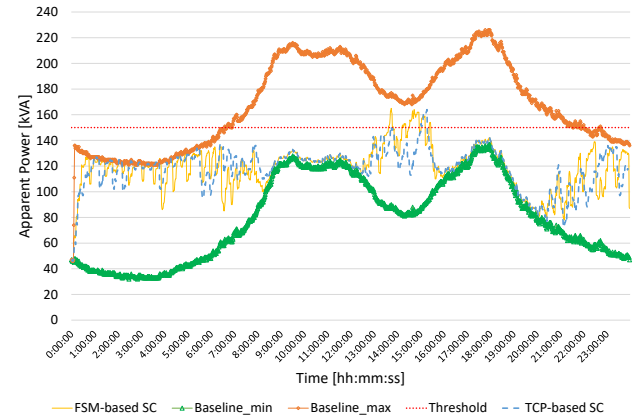


Figure 6: Apparent Power at the Transformer

with the TCP-like SC. As a result, the TCP-like SC prevents overloading at the transformer efficiently and contributes to a stable power quality of the grid in terms of assets overloading better than FSM-based SC.

5.2.3 Power allocation at charging stations. In any distributed system where multi processes share the same resource, a lot of attention should be paid to the starvation problem and the way of distributing the resource among the processes (i.e. Fairness). However, in the power grid this problem is more critical and hard to be addressed since the position of the CS plays a significant role by deciding how much power can be used. For example, the closer to the transformer, the fewer local power quality issues and more power can be used. As a result, the way of allocating the charging power among the CSs needs to be evaluated with taking into the consideration the significant role of the local operating conditions of each CS by determining the used charging power.

Figure 7 depicts the charging power allocated by the SCs and the total power utilized for smart EV charging. During peak hours of the day, the used power by each CS is at the minimum value. During off-peak hours, the typical saw-tooth pattern of C_{wnd} in the algorithm of TCP slow start can be seen; it is being reflected by the TCP-like SC in terms of charging power at each CS.

The CS connected at the critical node (C_2) is allocated limited power when compared to the other three CSs due to the voltage fluctuations at that point of the grid. During the first six hours of the day, the charging power is at maximum for C_1 , C_3 , and C_4 since fixing the voltage at the critical node needs only the reaction of C_2 . The charging power is reduced at all stations either when the situation hits warning or critical phases locally at any CS or reactions of the SC2 are not enough to keep the voltage of the critical point in the green range. For example, we can see that case in Figure 7 for the time between 06:00 AM and 08:00 AM

For more precise analysis, we calculate the energy distribution at each CS by performing area under the curve calculation using Figure 7. The total energy provided for CS using FSM-based SC is around 3% more than the case of using TCP-like SC. The reduced energy distribution value when using TCP-like SC is due to the higher level of reduction action taken by the controller during critical phases. The surpassing of TCP-like SC in terms of avoiding the transformer overloading provides further evidence in this respect. As we can see in Table 4, while the energy portion of C_2 during

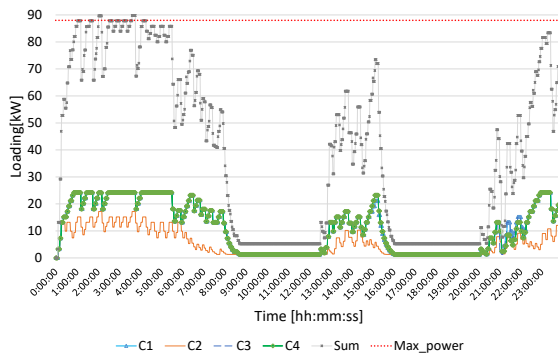


Figure 7: Charging power at four charging stations. Each colored line represent a CS. Grey is the sum power of all CSs and red line is rated maximum power of all CSs

FSM-based SC is 26.5% of the average energy distribution to other CSs, it is around 40% using TCP-like SC. We calculate the above percentage by dividing the energy of C_2 to the energy average of C_1 , C_3 , and C_4 .

Finally, we can conclude by observing the results that using TCP-like SC makes allocating more power to C_2 is possible by limiting the used power by other CSs, namely, C_1 , C_3 , and C_4 . The matching of power curves of C_1 , C_3 , and C_4 most of the time, which leads in its turn to the same amounts of consumed energy (see Figure 7 and Table 4), emphasizes the fairness of the proposed controller in the case no special local operating conditions take place, e.g., C_2 where the voltage criterion limits the used charging power. Otherwise, all the CSs will be able to use the same power all the time.

CS	FSM-based SC	TCP-like SC
C_1	51.20	39.91
C_2	13.39	16.24
C_3	51.48	41.00
C_4	48.46	40.92

Table 4: Energy Distribution in kWh among CSs between 12:30 and 16:00 O'clock.

5.2.4 OLTC-based solution vs. SC-based Solution. In this scenario, we assume that an OLTC transformer is used in the grid instead of the typical transformer. Using the OLTC, the adjustment of the voltage in the connected low-voltage grid can be done without performing further changes in the grid, particularly, no control on the CS demand. We repeat the aforementioned experiment with the $Baseline_{max}$ scenario and active OLTC. The tap changes based on the voltage level at the critical point in order to keep it in the green range all the time, however, by increasing or decreasing the tap position. It is significant to mention that OLTC is not designed to react directly to the overloading of the transformer. Nevertheless, the voltage of the high/low side of the transformer is the main metric for increasing or decreasing the tap position. In some cases, the impedance of the grid is considered as well. Finally, an additional voltage per tap is set to 2,8%.

As depicted in Figure 8, seven tap changes are required to keep the voltage of the critical point in the green range through the whole day; the highest tap position is zero and the lowest one is -2. The tap change from -1 to -2 is required only during the on-peak

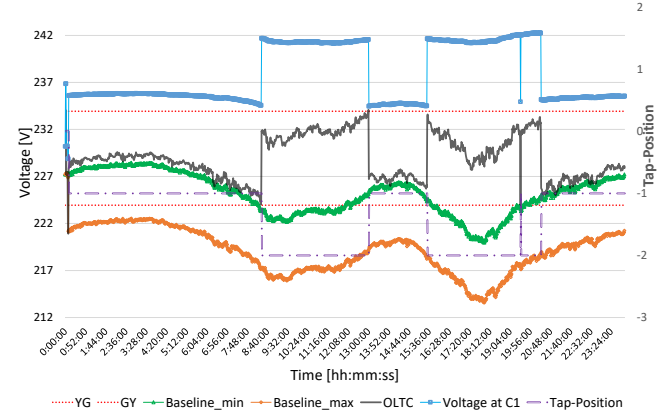


Figure 8: Voltage at C_1 and the critical point using OLTC

times, e.g., between 08:00 and 12:00. The voltage curve at the critical point using the OLTC transformer is even better than the one in the $Baseline_{Min}$. In the described scenario, where only one central OLTC transformer is used for connecting the low-voltage grid with an external medium-voltage grid, this scenario faces the downside that the OLTC only allows the regulation of the whole low-voltage grid. In case of high voltage discrepancies at different locations in the low-voltage grid exist, these discrepancies cannot be solved using only one central OLTC. For example, the voltage curve of C_1 (it is connected close to the transformer) becomes in yellow and red ranges all the time in contrast to the voltage of the critical point. That contradicts the design goals of the proposed system. To solve such cases, the installation of additional OLTCs or other Demand Side Management (DSM) and Supply Side Management (SSM) mechanisms might be necessary. Although OLTCs are great instruments for fast voltage regulation, grid operators may try to reduce the number of tap-changes to a minimum. The reason for this, as explained in [9], lies in the most common operational problem connected with OLTCs. This operational problem is that each tap-change causes physical stress to the transformer and therefore lowers its remaining expected lifetime.

6 CONCLUSION AND FUTURE WORK

In this work, a smart EV charger like TCP slow start is presented. Thanks to a notification mechanism about the grid status, that smart charger is able to react to two different events in the grid, namely, overloading the transformer and voltage drops on the feeder lines. The proposed SC shows the ability to drastically increase the quality of power with regard to the voltage level and load at the transformer by controlling the active power used by the CS. In comparison to other SC using the same notification mechanism, the TCP-like SC is fairer regarding the way of allocating the power at the CSs. Furthermore, we show the advantage of using a smart charging solution over an OLTC-based one in terms of the voltage control. In the future, the charger can be validated by PHIL in order to be ready for the real world application. Additionally, an evaluation using real mobility data can be performed, e.g., the German Mobility Panel (MOP). However, considering further factors of power quality beyond the voltage such as harmonics and unbalance of load can be seen as a promising direction even so existing hardware does not support those functionalities.

ACKNOWLEDGMENTS

The authors would like to thank Miss. Vaishali Byloor and Mr. Dominik Danner for their contribution to this work. Furthermore, this project has received funding from the European Union's Horizon 2020 research and innovation programme under grant agreement No. 713864 (ELECTRIFIC).



This project has received funding from the European Union's Horizon 2020 research and innovation programme under grant agreement No. 713864

REFERENCES

- [1] [n. d.]. AKKA Streams. Accessed on 03 May 2019. <http://doc.akka.io/docs/akka/current/java/stream/index.html>
- [2] [n. d.]. Reactive Streams. Accessed on 03 May 2019. <http://www.reactive-streams.org/>
- [3] M. Alonso, H. Amaris, J. Germain, and J. Galan. 2014. Optimal charging scheduling of electric vehicles in smart grids by heuristic algorithms. *Energies* 7, 4 (2014), 2449–2475. <https://doi.org/10.3390/en7042449>
- [4] A. Alyousef, D. Danner, F. Kupzog, and H. de Meer. 2018. Enhancing power quality in electrical distribution systems using a smart charging architecture. *Energy Informatics* 1, 1 (10 Oct 2018), 28. <https://doi.org/10.1186/s42162-018-0027-1>
- [5] O. Ardakanian, C. Rosenberg, and S. Keshav. 2012. RealTime Distributed Congestion Control for Electrical Vehicle Charging. *SIGMETRICS Perform. Eval. Rev.* 40, 3 (Jan. 2012), 38–42. <https://doi.org/10.1145/2425248.2425257>
- [6] O. Ardakanian, C. Rosenberg, and S. Keshav. 2013. Distributed control of electric vehicle charging. *Proceedings of the fourth international conference on Future energy systems - e-Energy '13* (2013), 101. <https://doi.org/10.1145/2487166.2487178>
- [7] BDEW Bundesverband der Energie- und Wasserwirtschaft e.V. 2013. BDEW Roadmap. Realistic Steps for the Implementation of Smart Grids in Germany. <https://www.bdew.de/energie/bdew-roadmap-smart-grids/> Accessed on 2nd of Jan. 2018.
- [8] C. Chung, J. Chynoweth, C. Chu, and R. Gadh. 2014. Master-Slave control scheme in electric vehicle smart charging infrastructure. *The Scientific World Journal* 2014 (2014).
- [9] A. Cichon, P. Fracz, and D. Zmarzly. 2011. Characteristic of acoustic signals generated by operation of on load tap changers. *Acta Physica Polonica A* 120, 4 (2011), 585–588.
- [10] David D Clark. 1995. The design philosophy of the DARPA internet protocols. *ACM SIGCOMM Computer Communication Review* 25, 1 (1995), 102–111.
- [11] Joaquim Delgado, Ricardo Faria, Pedro Moura, and Anibal T de Almeida. 2018. Impacts of plug-in electric vehicles in the portuguese electrical grid. *Transportation Research Part D: Transport and Environment* 62 (2018), 372–385. <https://doi.org/10.1016/j.trd.2018.03.005>
- [12] DIGSILENT. 2018. Digital Simulation and Network Calculation. www.digsilent.de/en/powerfactory.html Accessed on 20th of Dec. 2018.
- [13] EN Standard. 2010. 50160. *Voltage characteristics of public distribution systems* (2010), 18.
- [14] M. Faschang, F. Kupzog, R. Mosshammer, and A. Einfalt. 2013. Rapid control prototyping platform for networked smart grid systems. In *IECON 2013 - 39th Annual Conference of the IEEE Industrial Electronics Society*, 8172–8176. <https://doi.org/10.1109/IECON.2013.6700500> Accessed on 20th of Dec. 2018.
- [15] Apache Software Foundation. [n. d.]. Apache Kafka: A Distributed Streaming Platform. Accessed on 18 Jan 2019. <https://kafka.apache.org/>
- [16] Tanuja Ganu, Deva P Seetharam, Vijay Arya, Rajesh Kunnath, Jagabondhu Hazra, Saiful A Husain, Liyanage Chandratilake De Silva, and Shivkumar Kalyanaraman. 2012. nPlug: a smart plug for alleviating peak loads. In *Proceedings of the 3rd International Conference on Future Energy Systems: Where Energy, Computing and Communication Meet (e-Energy '12)*, ACM, New York, NY, USA, Article 30, 10 pages. <https://doi.org/10.1145/2208828.2208858>
- [17] V. Gupta, S. R. Konda, R. Kumar, and B. K. Panigrahi. 2018. Multiaggregator Collaborative Electric Vehicle Charge Scheduling Under Variable Energy Purchase and EV Cancellation Events. *IEEE Transactions on Industrial Informatics* 14, 7 (July 2018), 2894–2902. <https://doi.org/10.1109/TII.2017.2778762>
- [18] Y. He, B. Venkatesh, and L. Guan. 2012. Optimal Scheduling for Charging and Discharging of Electric Vehicles. *IEEE Transactions on Smart Grid* 3, 3 (Sep. 2012), 1095–1105.
- [19] L. Held, H. KrÄdmer, M. Zimmerlin, M. R. Suriyah, T. Leibfried, L. Ratajczak, S. Lossau, and M. Konermann. 2018. Dimensioning of battery storage as temporary equipment during grid reinforcement caused by electric vehicles. In *2018 53rd International Universities Power Engineering Conference (UPEC)*, 1–6. <https://doi.org/10.1109/UPEC.2018.8542035>
- [20] Van Jacobson. 1988. Congestion avoidance and control. In *ACM SIGCOMM computer communication review*, Vol. 18. ACM, 314–329.
- [21] L. Jian, Y. Zheng, and z. Shao. 2017. High efficient valley-filling strategy for centralized coordinated charging of large-scale electric vehicles. *Applied Energy* 186 (2017), 46–55.
- [22] F. Kong, X. Liu, Z. Sun, and Q. Wang. 2016. Smart Rate Control and Demand Balancing for Electric Vehicle Charging. In *2016 ACM/IEEE 7th International Conference on Cyber-Physical Systems (ICCCPS)*, IEEE, 1–10. <https://doi.org/10.1109/ICCCPS.2016.7479118>
- [23] Niels Leemput, Frederik Geth, Juan Van Roy, Pol Olivella-Rosell, Johan Driesen, and Andreas Sumper. 2015. MV and LV residential grid impact of combined slow and fast charging of electric vehicles. *Energies* 8, 3 (2015), 1760–1783.
- [24] Mingming Liu and SeÅan McLoone. 2015. Enhanced AIMD-based decentralized residential charging of EVs. *Transactions of the Institute of Measurement and Control* 37, 7 (2015), 853–867. <https://doi.org/10.1177/0142331213494100>
- [25] M. Longo, D. Zaminelli, F. Viola, P. Romano, R. Miceli, M. Caruso, and F. Pellitteri. 2016. Recharge stations: A review. In *2016 Eleventh International Conference on Ecological Vehicles and Renewable Energies (EVER)*, 1–8. <https://doi.org/10.1109/EVER.2016.7476390>
- [26] M Manbachi, A Sadu, H FarhangÄ, A Monti, A Palizban, F Ponci, and S Arzanzpour. 2016. Impact of EV penetration on Volt-VAR Optimization of distribution networks using real-time co-simulation monitoring platform. *Applied Energy* 169 (2016), 28–39.
- [27] Open Charge Alliance. 2017. OCPP 2.0. *OCPP Specification* (2017).
- [28] S. Paudyal, C. A. CaÄsÄzires, and K. Bhattacharya. 2011. Three-phase distribution OPF in smart grids: Optimality versus computational burden. In *2011 2nd IEEE PES International Conference and Exhibition on Innovative Smart Grid Technologies*, 1–7. <https://doi.org/10.1109/ISGTEurope.2011.6162628>
- [29] J. Rivera, C. Goebel, and H. Jacobsen. 2015. A Distributed Anytime Algorithm for Real-Time EV Charging Congestion Control. In *Proceedings of the 2015 ACM Sixth International Conference on Future Energy Systems - e-Energy '15*. ACM Press, New York, New York, USA, 67–76. <https://doi.org/10.1145/2768510.2768544>
- [30] S. Sharma, P. Jain, R. Bhakar, and P. P. Gupta. 2018. Time of Use Price based Vehicle to Grid Scheduling of Electric Vehicle Aggregator for Improved Market Operations. In *2018 IEEE Innovative Smart Grid Technologies - Asia (ISGT Asia)*, 1114–1119. <https://doi.org/10.1109/ISGT-Asia.2018.8467857>
- [31] M. Simonov. 2013. Event-driven communication in smart grid. *IEEE Communications Letters* 17, 6 (jun 2013), 1061–1064. <https://doi.org/10.1109/LCOMM.2013.043013.122798>
- [32] D Stahleder, D Reihls, M Nöhler, and F Lehfuß. 2018. Lablink-a novel cosimulation tool for the evaluation of large scale ev penetration focusing on local energy communities. In *to be presented in CIREN Workshop 2018*.
- [33] A. Stray, O. Clarke, D. Harvey, and O. Clarke. 2018. Electric vehicles and the digital revolution: an evolving legal landscape. <https://www.intelligenttransport.com/transport-articles/69187/evs-digital-revolution-legal/> Accessed on 17th of Jan. 2019.
- [34] J. Taft and P. De Martini. 2013. Ultra-large scale control architecture. In *2013 IEEE PES Innovative Smart Grid Technologies Conference (ISGT)*, 1–6. <https://doi.org/10.1109/ISGT.2013.6497906>
- [35] Tjarko Tjaden, Bergner Joseph, and Volker Quaschnig. 2015. Repräsentative elektrische Lastprofile für Wohngebäude in Deutschland auf 1-sekündiger Datenbasis. *HTW Berlin* November (2015), 8. <https://doi.org/10.13140/RG.2.1.5112.0080>
- [36] E. Ucer, M. C. Kisacikoglu, M. Yuksel, and A. C. Gurbuz. 2019. An Internet-Inspired Proportional Fair EV Charging Control Method. *IEEE Systems Journal* (2019), 1–11. <https://doi.org/10.1109/JSYST.2019.2903835>